A 2-D Test Problem for CFD Modeling Heat Transfer in Spent Fuel Transfer Cask Neutron Shields

G Zigh and J Solis
U.S. Nuclear Regulatory Commission

JA Fort
Pacific Northwest National Laboratory

Abstract

In the United States, commercial spent nuclear fuel is typically moved from spent fuel pools to outdoor dry storage pads within a transfer cask system that provides radiation shielding to protect personnel and the environment. The transfer casks are cylindrical steel enclosures with integral gamma and neutron radiation shields. Since the transfer cask system must be passively cooled, decay heat removal from the spent nuclear fuel canister is limited by the rate of heat transfer through the cask components and natural convection from the transfer cask surface. The primary mode of heat transfer within the transfer cask system is conduction, but some cask designs incorporate a liquid neutron shield tank surrounding the transfer cask structural shell. In these systems, accurate prediction of natural convection within the neutron shield tank is an important part of assessing the overall thermal performance.

The large-scale geometry of the neutron shield tank (typically an annulus ~2 meters in diameter but only 5-10 cm in thickness), and the relatively small scale velocities (typically <5 cm/s), represent a wide range of spatial and temporal scales that contribute to making this a challenging problem for computational fluid dynamics (CFD) modeling. Relevant experimental data at these scales are not available in the literature, although some recent modeling studies offer insights into numerical issues and solutions. However, in these studies and in the experimental data in the literature at smaller scales, the geometries have large annular gaps that are not prototypic of a transfer cask neutron shield.

This paper presents results for a simple 2-D problem that is an effective numerical analog for the neutron shield application. Because it is 2-D, solutions can be obtained relatively quickly allowing a comparison and assessment of sensitivity to model parameter changes. Turbulence models are considered as well as the tradeoff between steady state and transient solutions. Solutions are compared for two commercial CFD codes, FLUENT and STAR-CCM+. The results can be used to provide input to the CFD Best Practices for this application. Following study results for the 2-D test problem, a comparison of simulation results is provided for a high Rayleigh number experiment with large annular gap. Because the geometry of this validation is significantly different from the neutron shield, and due to the critical nature of this application, the argument is made for new experiments at representative scales.

1. INTRODUCTION

Transfer casks are part of the typical spent nuclear fuel transfer and storage system at a commercial nuclear power plant. Components include the dry storage canister (DSC), the transfer cask (TC) and a dry storage module. The DSC is designed to store multiple spent nuclear fuel assemblies. The transfer cask is used to move the DSC containing spent fuel assemblies from the spent fuel pool to the dry storage module. Loading and closure is performed with the DSC in the vertical orientation, and transfer to the storage module is typically in the horizontal

orientation. Loading of the DSC into the storage module can be either in the horizontal or vertical orientation depending on the system design. While the DSC is contained within the transfer cask, temperatures of the fuel within the canister are determined by the ability of the TC to transfer heat from the DSC to the surroundings. An integral part of the transfer cask design is the neutron shield, which in many designs consists of a liquid contained in an annular tank surrounding the TC structural shell. For horizontally oriented transfer casks, natural convection heat transfer within the liquid neutron shield can be an important means of transferring decay heat from the fuel assemblies to the environment. Appropriate estimates of that natural convection are therefore important in predicting thermal margins for this system.

Spent nuclear fuel storage systems are large and difficult to characterize in experiments. Because of this, computer models are most often used to support component design. In thermal performance predictions the convective heat transfer through the neutron shield is often characterized with a single overall effective heat transfer coefficient, or Nusselt number (Nu). This treatment may be adequate when heat transfer rate is relatively uniform around the cask circumference, or when low decay heat loading gives a large thermal margin and thus allows a large prediction uncertainty. However for systems closer to the thermal limit, it is important to consider variation in neutron shield heat transfer with angular position around the cask. This angular variation can be strongly affected by the configuration of the internal supports in the neutron shield tank. Regularly spaced axial supports that divide the annulus circumferentially into multiple isolated segments limit the extent of natural convection flow paths, restricting this mode of heat transfer primarily to the top and sides of the neutron shield, and limiting the lower segments of the annulus to mainly conduction only. In contrast, circumferential supports divide the annulus axially into annular segments within which natural convection is relatively unimpeded, since fluid can freely circulate around the neutron shield tank. (It should be noted, however, that in either configuration heat transfer at the bottom of the annulus is always limited to mainly conduction only due to thermal stratification with the higher temperature on the upper surface.)

For TC designs that use circumferential supports (Fig. 1), 3-D CFD models have shown that this configuration can lead to significant angular variation in heat transfer (Fort et al. 2010). Accurate prediction of the flow field and temperature distribution is essential to performance predictions for this case. The present study builds on the referenced 3-D study by examining solvers in greater depth with a wider variety of model settings. A simplified 2-D representation of a neutron shield is used for efficiency. Results are presented for two commercial CFD codes, FLUENT and STAR-CCM+. Following results with the test problem, these codes and solvers are applied to a high Rayleigh number experiment from the literature.

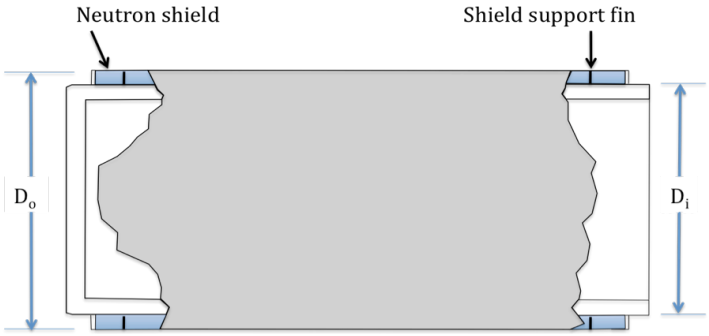

Figure 1: Transfer cask neutron shield with circumferential supports

2. TEST PROBLEM

The test problem considered in this study is a simplified, 2-D representation of the neutron shield studied by Fort et al (2010). The influence of the circumferential support fin is ignored, making this a 2-D problem. This case focuses on the fluid layer, ignoring heat transfer through the solid layers of the transfer cask, which can contribute to the overall circumferential non-uniformity in heat transfer rate. Symmetry is assumed about the vertical axis (coincident with the gravitational vector). This simplified test problem geometry is shown in Figure 2.

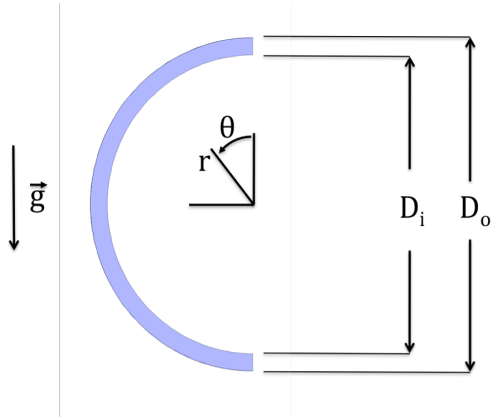

Figure 2: Test Problem Geometry

A uniform 1000 W/m^2 heat flux boundary condition is imposed at the neutron shield inner diameter. A uniform, 5 W/m^2-K convective boundary condition is applied at the outer diameter with thermal radiation to a 320 K ambient. Surface emissivity is 0.8. The neutron shield fluid is water.

Neutron shield dimensions are similar to those in the 3-D study. Inner diameter, D_i, is 2.1 m (82 in.) and outer diameter, D_o, is 2.3 m (91 in.). The neutron shield thickness is 12 cm (4.8 in.). The Rayleigh number, *Ra*, based on neutron shield thickness, *L*, is used to estimate flow regime, with transition to turbulent flow for $Ra_L > 10^9$ (Kreith, 2001). Using water properties at the expected bulk average temperature of 380 K (225°F) and a difference of 5 K in average temperature at the inner and outer diameters, Ra_L is calculated as follows:

$$Ra_L = \frac{g\beta\Delta T L^3}{\nu\alpha} = \frac{g\beta\Delta T L^3 \,\mathrm{Pr}}{v^2} \tag{1}$$

where *L* is the fluid layer thickness in the neutron shield

$$L = (D_o - D_i)/2 \tag{2}$$

thus Ra_L can be estimated as

$$Ra_L = \frac{9.81\mathrm{m/s^2}\left(1.01\times10^{-3}\,\mathrm{K^{-1}}\right)5\mathrm{K}\,(0.12\mathrm{m})^3\,1.1}{\left(\frac{185\times10^{-6}\,\mathrm{Pa\cdot s}}{919\mathrm{kg/m^3}}\right)^2} = 2.4\times10^9 \tag{3}$$

This result suggests that the flow field in the neutron shield annulus is in the turbulent regime.

Experiments have been performed for natural convection of liquids and gases between horizontal concentric cylinders. However, none have been performed for conditions that are close, in

geometry and Rayleigh number, to being prototypic of the conditions in the neutron shield[1]. Without an experiment for validation, computer model predictions must be viewed with care. Confidence in results can be improved through testing sensitivity to model input and by comparison with independent computer codes. It can also be strengthened by comparison of model results against experiments having similar physics. Both approaches are taken in this study.

3. 2-D TEST CASE

Results are given only for turbulent simulations, based on the estimated value of Ra_L in the turbulent range. The base case turbulence model is SST k-ω. Sensitivity to this turbulence model choice was investigated by comparison with a second commonly used model, low Reynolds number k-ε, but since it made no discernable difference for the cases tested, results are only included here for the base case. Results are presented for two solvers, segregated and coupled. Both transient and steady state (SS) simulations were considered. Comparisons between results for FLUENT and STAR-CCM+ are presented for several of these cases. Test cases are summarized in Table 1 along with the sub-section in which results will be discussed in Section 5.

Table 1: Cases Run

Turbulence Model	Solver	Run	Code	Discussed in Results Section
SST k-ω	Segregated	SS	FLUENT, STAR-CCM+	5.1
SST k-ω	Segregated	Transient	FLUENT, STAR-CCM+	5.2
SST k-ω	Coupled	SS	FLUENT, STAR-CCM+	5.3

The computational mesh is shown in Figure 3 and consists of 90 cells in the angular coordinate and 100 cells in the radial coordinate. The same mesh was used in all cases. Mesh spacing was condensed near the wall boundaries to capture the expected large near-wall velocity gradients for this high Rayleigh number flow and to have sufficiently small near wall mesh spacing to be compatible with a low-Reynolds number turbulence model.

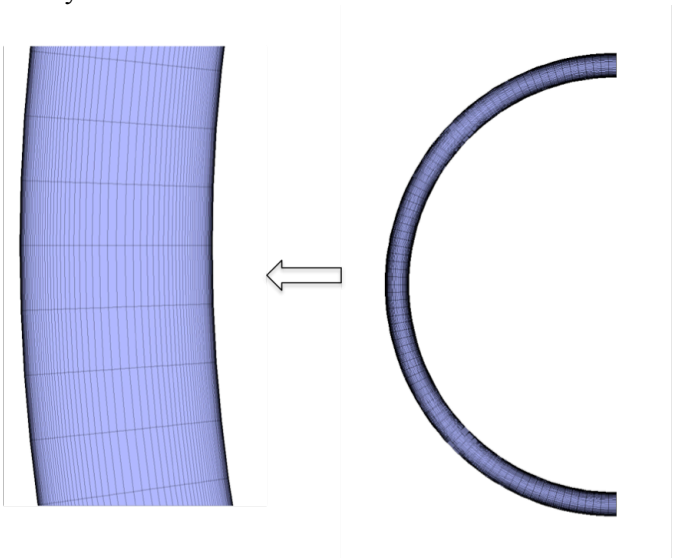

Figure 3: Computational Mesh

[1] A listing of experiments in the literature is provided in Fort et al, 2010.

4. CODES

Simulations were run using two codes, FLUENT ver. 6.3 and STAR-CCM+ ver. 4.06. These are representative examples of commercial CFD codes in use by the nuclear industry for fluid and thermal design and safety analysis. FLUENT is a product in the ANSYS suite of codes. STAR-CCM+ is a product of CD-adapco. The intent of this study was to compare results of the two codes using identical model options and solution parameters and identical descriptive inputs (geometry, boundary conditions and material properties). The process was aided by the ability of STAR-CCM+ to import mesh and boundary locations from models developed in FLUENT.

The primary difference between the codes that impacts this study is the different requirements for implementing the radiation boundary condition at the outer diameter. The model was initially developed in FLUENT, which allows a convective outer boundary with thermal radiation to be included on a 2-D (zero thickness) model. STAR-CCM+ requires a finite axial cell thickness to implement this boundary condition, and it must be on a solid. The 2-D FLUENT mesh was modified for use in STAR-CCM+ in order to replicate the thermal radiation boundary condition. The mesh was extruded to a finite thickness, and the outermost five cell layers were converted to solid. Since the thickness of this new solid layer was only 0.32 mm, or only 0.26% of the neutron shield thickness, this change was expected to have minimal effect in the comparison of results between the two codes.

5. RESULTS FOR 2-D TEST PROBLEM

Results are given in this section for the cases in Table 1. The segregated-solver steady-state case results are shown in Section 5.1. Results for the segregated-solver transient are provided in Section 5.2 and those for the coupled-solver steady state in Section 5.3.

Convergence was based on heat balance between the inner and outer boundary heat flux. Solution residuals were also monitored but would usually only decrease at the beginning stages of a simulation and then remain steady while heat balance was still far from converged. Agreement in heat balance within 2% was used as the initial criteria; actual results were within this bound but varied widely depending on the solver.

5.1 Segregated-solver Steady State

Solutions to the 2-D test problem using the segregated solver are described first for FLUENT. As this problem involved buoyancy driven flow, choice of momentum equations under-relaxation factor is important to obtain a well converged solution. At the start, under-relaxation factors were used, including a value of 0.7 for the momentum equation under-relaxation factor. Starting from isothermal condition as an initial guess to the temperature field, it took the solution close to 30k iterations to converge. Overall heat balance was used as the leading indicator to judge the convergence of the solution. The temperature difference between the inner hot wall and the outer cooler wall at the bottom ($\theta = 180°$ in Fig. 2) was used as an additional target variable to monitor the solution. A temperature difference of 8 K and heat imbalance of 0.062% were obtained as shown in Table 2 and Figure 4a, when a momentum under-relaxation of 0.7 was used. To improve the heat balance, the momentum under-relaxation factor was decreased from 0.7 to 0.1. Then, using the temperature field obtained from the 0.7 under-relaxation factor as an initial condition, a converged solution was obtained after an additional 30k iterations. As before, convergence of the solution was monitored using the heat imbalance between the inner and outer surfaces as well as the temperature difference between the two surfaces at the bottom (180°). A heat imbalance of 0.006% was calculated, and a temperature difference of 14 K was obtained at 180° as shown in Table 2 and Figure 4b. The outcome of this calculation was a wake-up call,

indicating that this problem is a challenge and careful choice of under-relaxation factor is a pre-requisite to obtain a good solution using the segregated solver. For example, in the problem modeled by Francis et al (2002) with a much larger diameter ratio, the authors found that an under-relaxation of 0.01 was required for Rayleigh numbers in excess of 10^9. So as the next step for the 2-D test problem, several smaller under-relaxation factors were chosen until values of target variables stayed unchanged as shown in Table 2. Under-relaxation values of 0.01 and 0.001 yielded comparable results for the target variables (temperature differences of 22 and 23 K, respectively and negligibly small heat imbalance). The results from using an under-relaxation factor of either 0.01 or 0.001 were satisfactory. Plots of boundary temperatures for these two under-relaxation factors are shown in Figures 4c and 4d.

Table 2: Convergence Metrics for Varied Momentum Under-relaxation with FLUENT

Momentum Under-relaxation	Heat Balance (%)	Tmax (K)	Tmin (K)	Peak Vmag (cm/s)	ΔTbottom (K)
0.7	0.062	395	374	1.71	8
0.1	0.006	399	373	1.83	14
0.01	0.0017	400	360	2.38	22
0.001	0.0002	400	360	1.85	23

A similar process repeated with STAR-CCM+ produced nearly equal results. Velocity under-relaxation is the only parameter that needs to be changed from its default value in STAR-CCM+. A temperature-dependent density was used in this case with no apparent adverse impact in solution residuals. However, more iterations were required than in the FLUENT simulations to reach steady state. This slower convergence is due to the previously mentioned differences in the STAR-CCM+ model required to impose a thermal radiation boundary condition at the outer wall. (In a test case run without thermal radiation, both codes converged at the same rate.) Simulations with STAR-CCM+ were each initialized with zero velocity and uniform temperature and then run for 120k iterations, except for the lowest under-relaxation case (0.001) which required 240k iterations to converge. Table 3 lists results for the conditions tested. Boundary temperature distributions at the momentum under-relaxation of 0.001 are close to the FLUENT results in Figure 4c. In the STAR-CCM+ simulation at the lowest under-relaxation, the minimum temperature continued to vary after the maximum temperature reached and maintained a steady value. Over the initial 30k iterations, the minimum temperature varied between 360-363 K. Despite that, the lowest under relaxation results for each code, as shown in Tables 2 and 3, have maximum temperatures within 1 K, minimum temperatures within 2 K, and temperature differences at the bottom within 1 K.

Table 3: Convergence Metrics for Varied Momentum Under-relaxation with STAR-CCM+

Velocity Under-relaxation	Heat Balance (%)	Tmax (K)	Tmin (K)	Peak Vmag (cm/s)	ΔTbottom (K)
0.7	0.66	397	372	1.86	14
0.3	0.82	398	367	1.9	17
0.01	0.45	399	362	1.9	21
0.001	0.03	400	361	2.2	22

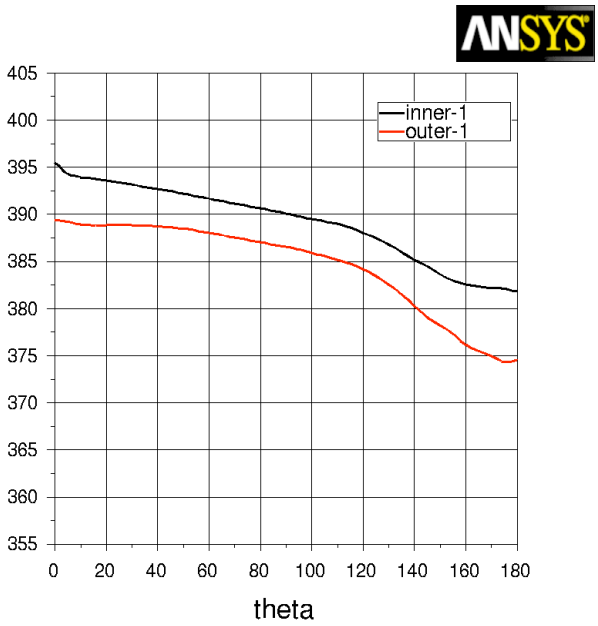

Figure 4a: Boundary temperature (K) for segregated solver steady state (momentum under-relaxation = 0.7)

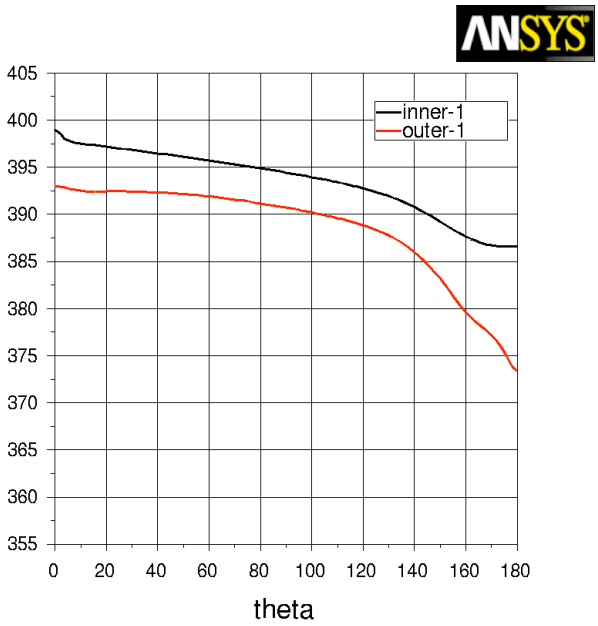

Figure 4b: Boundary temperature (K) for segregated solver steady state (momentum under-relaxation = 0.1)

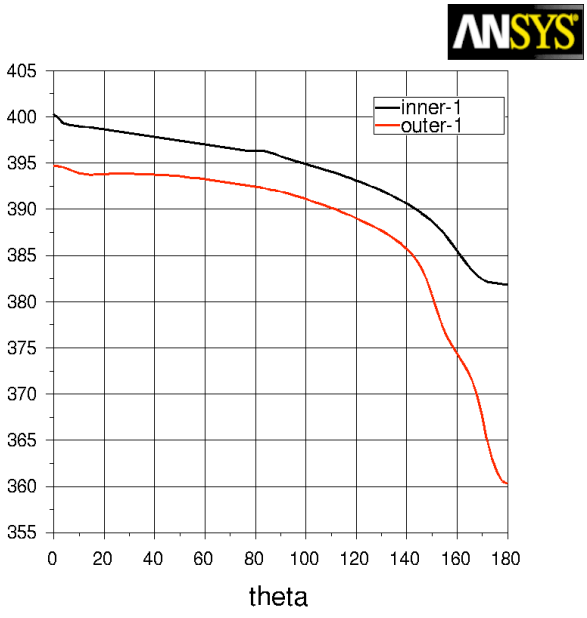

Figure 4c: Boundary temperature (K) for segregated solver steady state (momentum under-relaxation = 0.01)

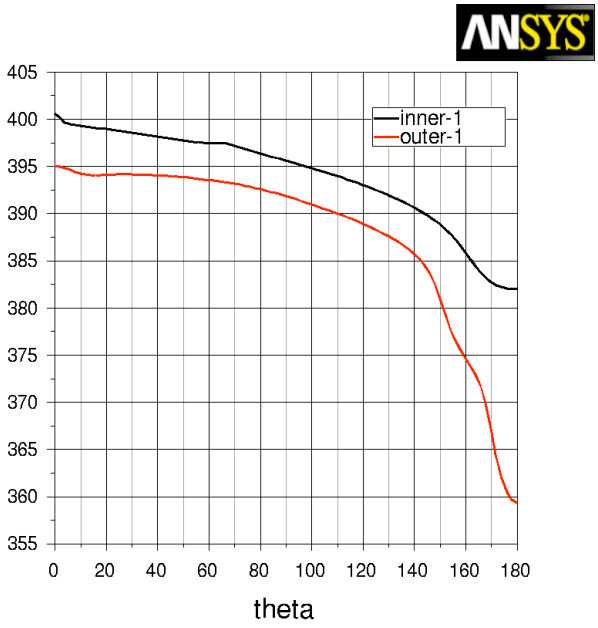

Figure 4d: Boundary temperature (K) for segregated solver steady state (momentum under-relaxation = 0.001)

5.2 Segregated-solver Transient

It is always prudent to check a natural convection problem with a transient solution, since the flow field may actually be physically unsteady. While it takes significantly more computational effort, the transient mode captures unsteady features that can be averaged out in the steady state. This case used the same solver and turbulence model that was used in the steady state simulation described in the previous case (momentum under-relaxation in the transient was kept at the default value of 0.7). This case was run with both codes.

For the segregated solver transient simulation in FLUENT, ¼ of the characteristic time was used as the time step. The time characteristic of 1.3 sec was calculated based on the Rayleigh number.

The characteristic time in buoyancy driven flow can be written as:

$$\tau = \frac{L}{U} \sim \frac{L^2}{\alpha}(\mathrm{Pr}\,Ra)^{-1/2} = \frac{L}{\sqrt{g\beta\Delta TL}}$$

where L and U are characteristic length and velocity, α is thermal diffusivity, Pr is Prandtl Number, Ra is Rayleigh Number, β is thermal expansion coefficient and ΔT is the temperature gradient.

$$\Delta t \approx \frac{\tau}{4}$$

Using a larger time step may lead to divergence. After the oscillations with a typical frequency of $f\tau = 0.05 - 0.09$ have decayed, the solution reaches steady state (i.e. f and τ are the oscillation frequency in Hz and the time constant, respectively). The solution may take as many as 5000 time steps to reach steady state.

Results shown for the FLUENT segregated solver transient in Table 4 indicate a value of 23 K for the temperature difference between the two plates at 180°. This is within 1 K of the value of the target variable obtained for both codes with the segregated solver steady state (Tables 2 and 3). The boundary temperature profiles are nearly identical to those for the lower under-relaxation segregated solver steady-state results in Figures 4c and 4d.

For STAR-CCM+, the simulation was initialized with the initial (α = 0.7) segregated-solver steady-state solution and was advanced with a constant time step of 0.1s, which gave a peak CFL of 1.5. The simulation was run until temperature extremes were no longer changing and thermal equilibrium was again established. The run was stopped after 11 hours of simulated time. At that point the difference between inner and outer boundary heat flux was 5 W (1.9% of total). Predicted maximum and minimum temperatures for this case were 399 K and 347 K, respectively. In comparison to the FLUENT segregated-solver transient result, the 399 K maximum temperature is within 1 K but the 347 K minimum is 16 K lower. The 37 K temperature difference at the bottom is likewise considerably greater than that observed in the FLUENT transient. These same differences are observed between the STAR-CCM+ transient and the segregated-solver steady-state results for both codes (Tables 2 and 3). The predicted peak fluid velocity of 1.9 cm/s is the same as in the STAR-CCM+ segregated-solver steady state (Table 3). Potential reasons for these differences are discussed in Section 5.4.

Table 4: Segregated-solver transient results

Code	Heat Balance (%)	Tmax (K)	Tmin (K)	Peak Vmag (cm/s)	ΔTbottom (K)
FLUENT	0.022	398	363	1.76	23
STAR-CCM+	0.82	399	347	1.9	37

5.3 Coupled-solver Steady State

The next case run was a steady-state solution with the coupled solver. This case was run with both codes. The coupled solvers in FLUENT and STAR-CCM+ appear equivalent, referencing the same literature and having similar controls. However, the implementations undoubtedly have differences. A CFL number is the primary user-input to the solver. For both codes, the default starting point is a CFL of 5, which can be adjusted upward to speed the solution to convergence. For the FLUENT simulation, the CFL was kept constant at the default value. The solution was converged at 100k iterations with a heat balance of less than 0.07%. For STAR-CCM+, the CFL adjusted to 10, 50 and 100 at iteration counts of 22k, 35k and 50k, respectively. The STAR-CCM+ solution converged much more slowly. Heat balance was within 1% at 750k iterations and by 1.2M iterations was down to 0.5%, at which point the simulation was stopped.

Results for simulations with both codes are shown in Table 5. The predicted maximum and minimum temperatures for this case were: 396 K and 360 K for FLUENT, and 400 K and 348 K for STAR-CCM+. These results for FLUENT are consistent with the segregated-solver steady state and segregated-solver transient results for the same code (Tables 2 and 4, respectively). For STAR-CCM+ these results are consistent with results of the STAR-CCM+ transient (Table 4). Velocity magnitudes compare reasonably well between solver options. The peak velocity from the FLUENT coupled solver steady state was 1.97 cm/s, and the peak velocity from the same solver in STAR-CCM+ was 1.9 cm/s, so these are within +/- 0.1 cm/s of the other solver predictions of 1.9 cm/s.

Table 5: Coupled-solver steady-state results

Code	Heat Balance (%)	Tmax (K)	Tmin (K)	Peak Vmag (cm/s)	ΔTbottom (K)
FLUENT	0.07	396	360	1.97	22
STAR-CCM+	0.5	400	348	2.0	32

5.4 Which solver to choose?

One objective of this study was to recommend the most appropriate solver for the neutron shield application. A summary of results by case is provided in Table 6. For FLUENT, the coupled-solver steady state gave minimum and maximum temperatures that agree within 3 K with the segregated-solver steady state and segregated-solver transient solutions with the same code. Agreement was even better (22 ± 1 K) for the target variable of temperature difference between the two boundary temperatures at 180° obtained using the transient solver. The agreement of both the coupled solution and the transient solution verifies that the results obtained for the segregated solver with under-relaxation of both 0.01 and 0.001 are satisfactory.

For STAR-CCM+, the result is less clear. The coupled-solver steady state agrees closely with the segregated-solver transient for the same code. The fact that both differ from the STAR-CCM+ segregated-solver steady state results as well as the FLUENT results is a concern, and the cause has not been determined. It could be due to differences in model implementations in the two codes (recall the discussion in Section 3 about the radiation boundary condition and cells converted to solids). However, the level of agreement between STAR-CCM+ and FLUENT segregated-solver steady-state results argue against this. The model implementations are the same for all solver options tested with each code, and results with each code should be consistent. The reason this is not achieved with STAR-CCM+ is not yet explained, and additional work is needed to establish the cause and means by which consistent results can be obtained.

For the FLUENT runs, the important result here is that, with a given implementation of this test problem, consistent results can be produced with different solver options. While that may seem like an obvious expectation, it has been shown in this paper that it sometimes takes some effort to do so.

Table 6: Summary of simulation results

Case	Code	Tmax (K)	Tmin (K)	Peak Vmag (cm/s)	ΔTbottom (K)
Segregated-solver steady state	FLUENT	400	360	1.85	23
	STAR-CCM+	400	361	2.2	22
Segregated-solver transient	FLUENT	398	363	1.76	23
	STAR-CCM+	399	347	1.9	37
Coupled-solver steady state	FLUENT	396	360	1.97	22
	STAR-CCM+	400	348	2.0	32

If consistent results can be obtained between different solvers for a given code, which solver should be used? The answer to this question must consider both tradeoffs and reliability. The segregated solver shows a clear benefit in run times, producing consistent results once under-relaxation parameters were small enough. The coupled solvers for both codes were straightforward to use, produced consistent results, and did not suffer the long run times required for the transient. Moreover, the coupled solver results were produced with a single simulation. The speed of the segregated-solver steady state is of less benefit when, as has been shown, multiple simulations must be run to confirm a converged solution.

The final choice depends on the situation. A one-off analysis would suggest the more reliable coupled solver, whereas small changes to a well understood design may be modeled more efficiently with a segregated-solver steady state using known run parameters. Clearly all situations benefit from independent runs with a different solver or with changes in input or run conditions to examine sensitivity of results. The option to run two separate codes is even better but is understood to rarely be an option.

6. RESULTS FOR COMPARISON WITH EXPERIMENT

It was acknowledged earlier that there are no comparable experimental datasets for the neutron shield application. Specifically, there are no experiments that feature both a comparable diameter ratio (imposing a thin gap thickness) and sufficiently high Rayleigh number. However, there do exist large-gap experiments at comparable Rayleigh number. The experiment of McLeod and Bishop (1989) was selected for model comparison, specifically their case for a Rayleigh number

of 1×10^9. A similar comparison was attempted by Desai and Vafai (1994). This is the only comparison that can be found. One drawback of using this comparison is that the diameter ratio is higher than in the problem we are dealing with (i.e. radius ratio 4.85 as compared to 1.15 in the neutron shielding problem). Constant temperatures were used in this experiment at the inner and outer cylinder, and these are used as boundary conditions on the simulation.

FLUENT was used to run this case using segregated and coupled steady state solvers, as well as transient solver. The convergence of the segregated solver steady state was not affected by the choice of momentum under-relaxation factor. Both the momentum under-relaxation factor of 0.3 and 0.01 gave comparable results, as show in Figures 5a and 5b. The results from the segregated solver were identical to the transient solution shown in Figure 5d. For the transient solution, ¼ of the characteristic time was used as the time step. The time characteristic was calculated based on the Rayleigh number similar to the neutron shield transient case discussed above. The coupled solver seems to fit the experimental data a little better at the 0 degree location (top of the annulus), as shown in Figure 5c.

This case was also run using STAR-CCM+ with both the segregated and coupled steady state solvers and with the segregated transient solver. The segregated solver and coupled solver produced equivalent results and plots of cross-gap appear almost identical to the FLUENT segregated steady state solution in Fig. 5b. The STAR-CCM+ segregated solver steady state was run with a momentum under-relaxation of 0.01. The STAR-CCM+ transient was run with a full 360° mesh so that the symmetry boundary condition would not limit potential unsteady effects. The plume position was seen to oscillate laterally near the top of the inner cylinder, which also affected the plume location near the outer cylinder. However, an oscillation frequency was not determined.

No uncertainty (i.e. error bars) was reported for the experimental data concerning the placement of the thermocouples or any other uncertainties that can influence the data. To investigate the effect of uncertainty introduced by thermocouple locations, an additional plot for 1 and 2 degrees are shown in Figure 6. As seen in the Figure, an angle of 1 degree can make a difference in results comparison, and the results obtained at 2 degrees matched the experimental data very well.

Sensitivity to model choices, for example the choice of turbulence model, was not investigated and could also be important. The lack of agreement at the top of the neutron shield (0°) is possibly due to unsteady behavior in the plume, and inadequate treatment of turbulent fluid mixing in the models used.

The experiment used constant temperature walls, so that the temperature difference between the inner and outer cylinder is kept constant. To investigate the effect of the boundary condition on simulation results, additional runs were performed. These additional runs were intended to determine if temperature difference between the inner and outer cylinders in the validation case with higher radius ratio behaves similarly as in the neutron shielding case with lower radius ratio. To do so, using the validation configuration, constant heat of 8100 W/m^2 was applied at the inner cylinder. At the outer cylinder mixed boundary conditions including both convection and radiation to a surrounding temperature of 300 K was used. Both segregated as well as coupled solvers were chosen to perform the simulations. All three solvers performed similarly as shown in Figure 7. As expected the two problems behave differently. The behavior of the temperature difference seen in the neutron shielding is due to the smaller gap (i.e. small radius ratio). The increase in temperature difference between the two cylinders in the bottom of the gap is a phenomenon that is present in the small radius ratio and not in the large gap (i.e. large radius ratio).

The latter sets of runs demonstrated that the physics in the smaller radius ratio gap (as in the neutron shielding) and in the large radius ratio of the experiment are different. As such, experiments for small radius ratio are needed to perform validation for this type of problem.

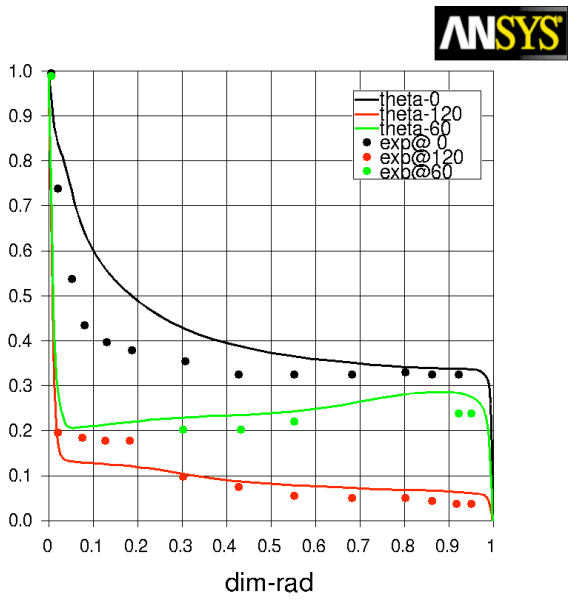

a. segregated-solver steady state (momentum under-relaxation = 0.3)

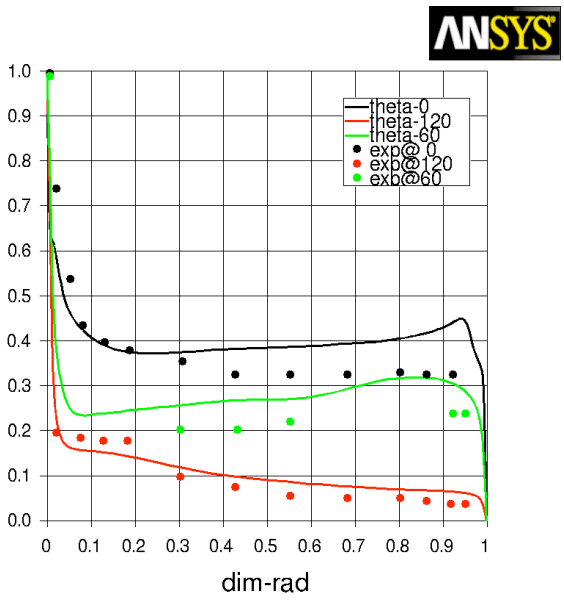

c. coupled-solver steady state

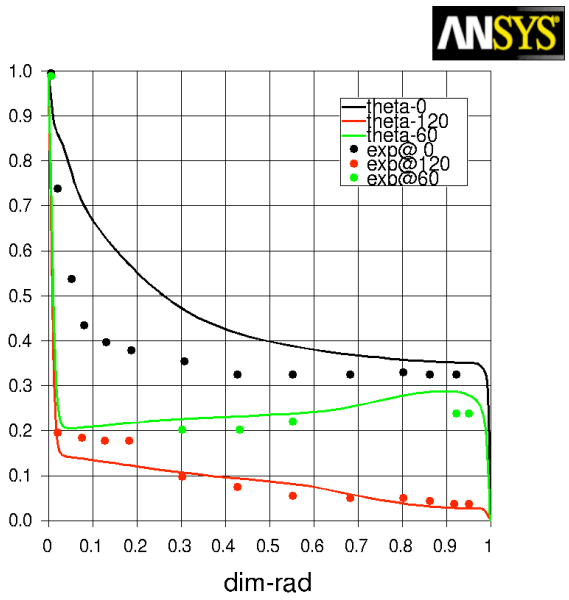

b. segregated-solver steady state (momentum under-relaxation = 0.01)

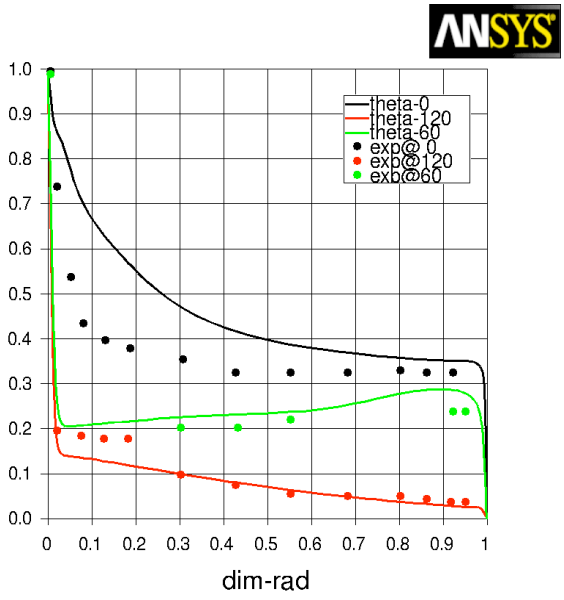

d. segregated-solver transient

Figure 5: Cross-gap temperature profiles for FLUENT simulations (comparison with Fig. 5 of McLeod and Bishop, 1989)

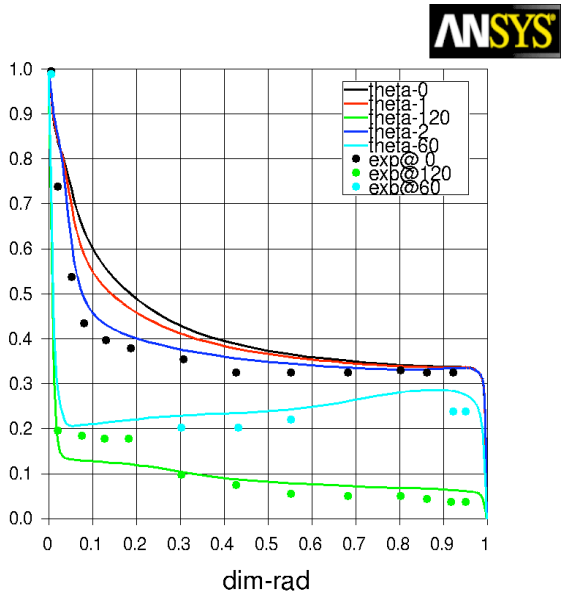

Figure 6: Cross-gap temperature profiles for FLUENT simulations (comparison with Fig. 5 of McLeod and Bishop, 1989) where 1° and 2° profiles reflect sensitivity to measurement position

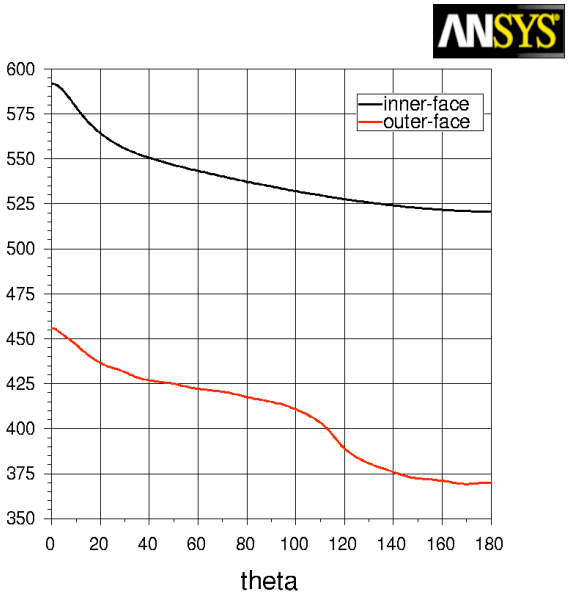

a. segregated-solver steady state (momentum under-relaxation = 0.7)

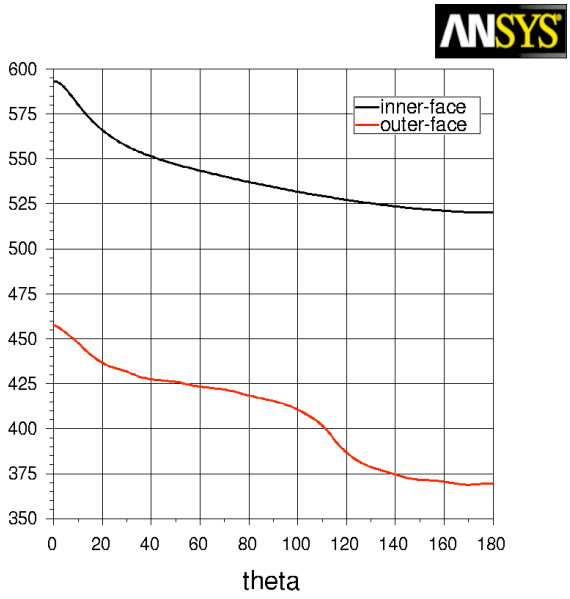

b. segregated-solver steady state (momentum under-relaxation = 0.01)

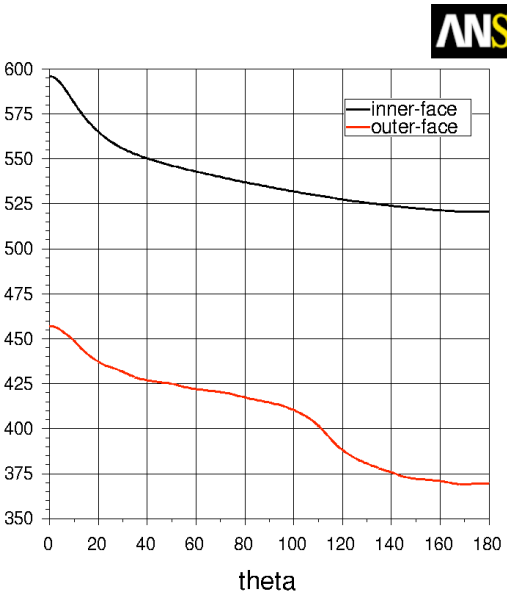

c. coupled-solver steady state

Figure 7: Boundary surface temperature profiles for FLUENT simulations showing effect of constant heat flux boundary condition for same geometry as experiment

7. CONCLUSIONS

Results obtained with the 2-D model are consistent with those observed for the 3-D model, which included a support fin (Fort et al, 2010). FLUENT and STAR-CCM+ segregated-solver steady-state results compare well for the same conditions. Segregated-solver transient and coupled-solver steady-state results for FLUENT are consistent with segregated-solver steady-state results with both codes. However, there was significant difference in results produced using the segregated-solver transient and coupled-solver steady state in STAR-CCM+. The cause of this difference is as yet unresolved.

Regarding the choice between solvers, the segregated-solver steady state is computationally efficient and can give consistent results in both codes, but it does require a careful evaluation process to ensure an accurate solution. The coupled-solver steady state is straightforward to use and gave consistent results without the large penalty in run time associated with the transient. The coupled-solver steady state is the recommended solution approach for this problem.

While experimental data is not available in the literature for natural convection in horizontal concentric cylindrical annuli with small radius ratios and Rayleigh number typical of the neutron shield application, good agreement was shown for both codes against experimental data for a large radius ratio geometry with similar Rayleigh number. Simulations demonstrated that the physics in the smaller radius ratio gap (as in the neutron shielding) and the large radius ratio in the experiment are different. Experiments for small radius ratio are needed to perform validation for this type of problem.

REFERENCES

Anon., *ANSYS FLUENT 12.0, Users Guide*, Canonsburg, PA, April 2009.

Anon., *User Guide, STAR-CCM+ Version 4.06.011*. CD-adapco, Melville, NY, 2009.

Desai, C. P. and K. Vafai, "An investigation and comparative analysis of two- and three-dimensional turbulent natural convection in a horizontal annulus", *Int. J. Heat and Mass Transfer*, **37**, no. 16, pp. 2475-2504, 1994.

Fort, JA, JM Cuta, CJ Bajwa and E Baglietto, "Modeling Heat Transfer in Spent Fuel Transfer Cask Neutron Shields - A Challenging Problem in Natural Convection", in Proceedings of ASME 2010 PVP.

Francis, Nicholas D., Jr. et al., CFD Calculation of Internal Natural Convection in the Annulus between Horizontal Concentric Cylinders, SAND2002-3132, Sandia National Laboratories, 2002.

Kreith, F. and M. S. Bohn, *Principles of Heat Transfer*, 6th edition, Brooks/Cole, Pacific Grove, CA, 2001.

McLeod, A. E. and E. H. Bishop, "Turbulent natural convection of gases in horizontal cylindrical annuli at cryogenic temperatures", *Int. J. Heat and Mass Transfer*, **32**, no. 10, pp. 1967-1978, 1989.